

Bandwidth-Efficient Communication through 225 MHz Ka-band Relay Satellite Channel

Joseph A. Downey*, James M. Downey†, Richard C. Reinhart*, Michael A. Evans‡
and Dale J. Mortensen§

NASA Glenn Research Center, Cleveland, OH, 44135

The communications and navigation space infrastructure of the National Aeronautics and Space Administration (NASA) consists of a constellation of relay satellites (called Tracking and Data Relay Satellites (TDRS)) and a global set of ground stations to receive and deliver data to researchers around the world from mission spacecraft throughout the solar system. Planning is underway to enhance and transform the infrastructure over the coming decade. Key to the upgrade will be the simultaneous and efficient use of relay transponders to minimize cost and operations while supporting science and exploration spacecraft. Efficient use of transponders necessitates bandwidth efficient communications to best use and maximize data throughput within the allocated spectrum. Experiments conducted with NASA's Space Communication and Navigation (SCaN) Testbed on the International Space Station provides a unique opportunity to evaluate advanced communication techniques, such as bandwidth-efficient modulations, in an operational flight system. Demonstrations of these new techniques in realistic flight conditions provides critical experience and reduces the risk of using these techniques in future missions. Efficient use of spectrum is enabled by using high-order modulations coupled with efficient forward error correction codes. This paper presents a high-rate, bandwidth-efficient waveform operating over the 225 MHz Ka-band service of the TDRS System (TDRSS). The testing explores the application of Gaussian Minimum Shift Keying (GMSK), 2/4/8-phase shift keying (PSK) and 16/32- amplitude PSK (APSK) providing over three bits-per-second-per-Hertz (3 b/s/Hz) modulation combined with various LDPC encoding rates to maximize throughput. With a symbol rate of 200 Mbaud, coded data rates of 1000 Mbps were tested in the laboratory and up to 800 Mbps over the TDRS 225 MHz channel. This paper will present on the high-rate waveform design, channel characteristics, performance results, compensation techniques for filtering and equalization, and architecture considerations going forward for efficient use of NASA's infrastructure.

I. Introduction

NATIONAL Aeronautics and Space Administration (NASA)'s communication networks have historically been optimized for operating in the power-limited region of the channel capacity curve. In those regions, BPSK/QPSK modulations are preferred, and they are usually paired with a low rate Turbo code or convolutional code. Due to an ever-increasing desire for more science data and the limited available spectrum, future missions will need to operate in the bandwidth-limited region. Examples of bandwidth-efficient techniques include high-order modulations (8-PSK, 16-APSK), modern forward error correction (LDPC with code rates greater than 1/2), and careful pulse-shaping (e.g. square-root raised cosine (SRRC)). These techniques present different challenges to the design of a communication system, in terms of the required signal-to-noise ratio, implementation complexity, and allowing for non-zero peak-to-average power ratios. For example, signals with high peak-to-average power ratios are heavily distorted by non-linear devices,

*Telecommunications Engineer, Information and Signal Processing Branch, Non-member.

†Electronics Engineer, Advanced High-Frequency Branch, Non-member.

‡Computer Engineer, Information and Signal Processing Branch, Non-member.

§Telecommunications Engineer, Architectures, Networks and Systems Integration Branch, Non-member

such as traveling wave-tube amplifiers (TWTAs). On typical spacecraft these amplifiers are operated near saturation to maximize power efficiency, where the distortion is most severe.

Glenn Research Center has developed a capability to support various waveforms using the Space Communication and Navigation (SCaN) Testbed that is currently operating on the International Space Station (ISS). The *Reconfigurable Bandwidth-Efficient Waveform for High-Rate Telemetry* was developed by NASA as part of an experiment to demonstrate high-rate waveforms through the Space Network. The goal of the experiment is to maximize the throughput over the Ka-band Single Access service using the 225 MHz channel.

The rest of this paper is organized as follows. In Section II the overall relay satellite system is described. In Sections III and IV the baseline and bandwidth-efficient waveforms are presented. Test and technology objectives are contained in Section V. Methods to perform non-linear channel compensation (digital pre-distortion) are identified in Section VI. The results of laboratory and on-orbit testing are detailed and summarized in Section VII. Finally, future work and conclusions are in Sections VIII and IX.

II. Ka-band Relay Satellite System Description

The NASA Space Communications and Navigation (SCaN) Program is responsible for providing communications and navigation services to space flight missions throughout the solar system. The SCaN Testbed is an advanced integrated communications system and laboratory installed on the ISS, and has been operating experiments with multiple software defined radios (SDRs) since 2012.^{1,2} The SDRs are reprogrammable and can run reconfigurable waveform applications.^{3,4} Figure 1 shows the payload enclosure and the various antenna locations and each of the three software defined radios. There are five antennas around the system; three S-band, one Ka-band, and one L-band (Global Positioning Satellite). This experiment uses the Harris Ka-band SDR,⁴ high-efficiency TWTAs,⁵ and the 0.5 m high-gain (39 dBi) antenna.

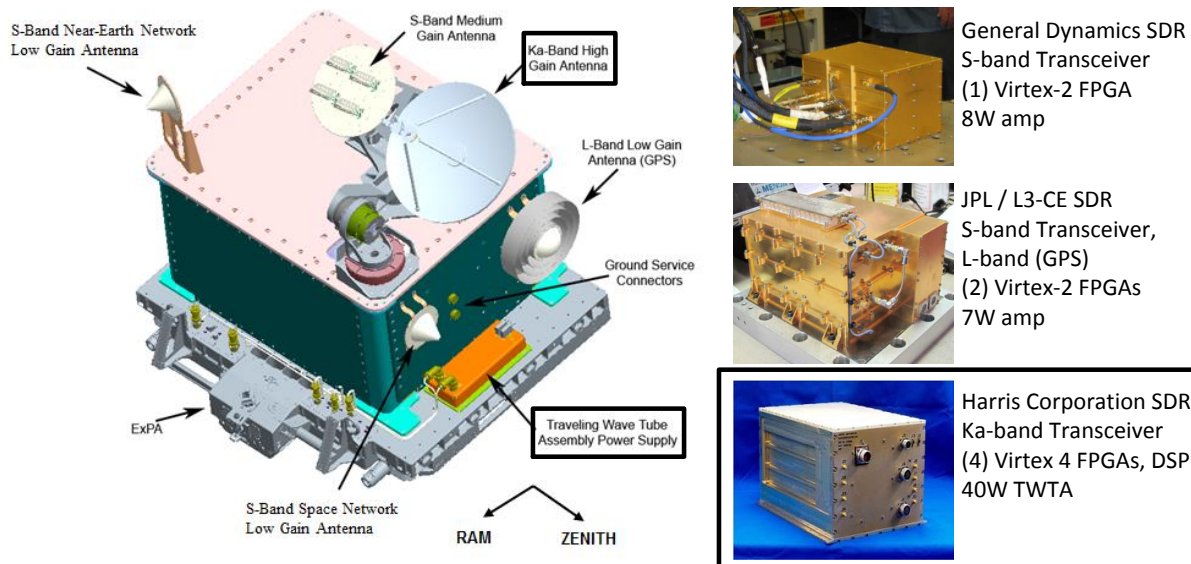


Figure 1. SCaN Testbed

The relay satellite test scenario is shown in Figure 2. The Ka-band signal from SCaN Testbed to TDRS is received, amplified, and downlinked over Ku-band to the relay satellite ground station at the White Sands Complex (WSC), in White Sands, New Mexico. A 370 MHz intermediate frequency (IF) service is used to route the received signal from the ground station to the local user equipment, which includes several high data-rate receivers. Additional equipment includes a wideband signal analyzer, which is used for spectral and vector signal analysis. The SCaN Testbed Ka-band antenna pointing system was configured in auto-track mode, an in-house developed closed-loop antenna pointing system. Although the TDRS system offers its own closed-loop tracking (auto-track) during standard operations, the auto-track service is not available

when using the IF service because it does not have the necessary feedback from the receiver. However, the program track mode (open-loop pointing) of TDRS is able to provide sufficient pointing accuracy for this experiment.

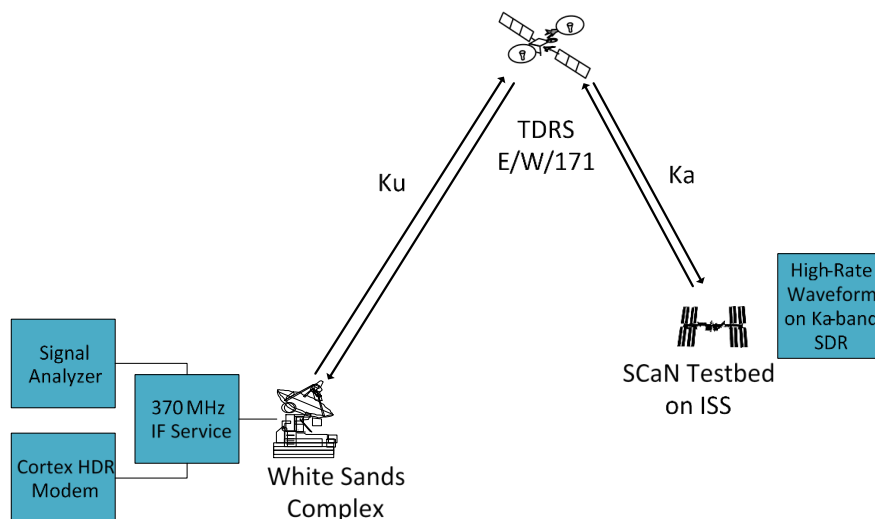


Figure 2. Ka-band Relay Satellite System.

A simplified link budget for this scenario is shown in Table 1. In this relay satellite system, the overall C/N_0 performance is dominated by the Ka-band link between the user spacecraft and TDRS. In TDRS program track mode the specified minimum G/T of the relay satellite is 23 dB/K, while the auto-track performance is 3.5 dB higher (26.5 dB/K).⁶ In practice, the actual program track performance exceeded its specification for typical SCaN Testbed events, and was closer to the specified auto-track performance. Depending on the specific TDRS antenna, polarization, and channel assignment, actual TDRS G/T values can exceed the specification by several dB.⁷ Thus, the net C/N_0 in Table 1 is conservative.

Table 1. Link Budget.

Parameter	Value	Notes
Frequency (GHz)	25.65	
Transmit Power (dBW)	16.24	
Transmit Circuit Loss (dB)	-2.55	
Antenna Gain (dBi)	39.06	Including 0.2 dB pointing loss
EIRP (dBW)	52.75	
Free Space Loss (dB)	-212.45	44.5 degree elevation
Misc Losses (dB)	-0.14	Polarization mismatch
Received Isotropic Power (dBW)	-159.83	
TDRS G/T (dB/K)	23	LEO program track specification *
Boltzmann's Constant	-228.6 dBW/K/Hz	
C/N_0 at TDRS (dB-Hz)	91.77	
TDRS Ku-band Downlink C/N_0 (dB-Hz)	110.5	Clear sky
Net C/N_0 at Ground (dB-Hz)	91.71	Parallel channel calculation

* Space Network User's Guide Rev 10.

The current high-rate receivers available via the Space Network Ka-band Single Access service do not support high-order modulations, LDPC decoding, or data rates above 300 Mbps. Instead, for this experiment commercial receivers were used, which were available from a project upgrading the ground receivers at WSC called the User Service Subsystem Component Replacement (USS-CR) Project.⁸ The USS-CR Wideband (WB) demodulator is a T1200 High Rate Receiver, developed by RT Logic. In addition, a commercial high-rate modem built by Zodiac Data Systems, the Cortex XXL HDR, part of the GRC-provided measurement system was also used for performance comparison, and for operation with high-order modulation formats such as 16/32-APSK, unavailable on the USS-CR receiver.

III. Baseline Waveform

Historically NASA missions have used lower order modulations at high symbol rates. While not bandwidth efficient, the approach is simpler and least affected by non-linearities in the system. The baseline waveform for the SCA_N Testbed Ka-band SDR is an offset-QPSK (OQPSK) modulation with a rate 1/2 convolutional code. This waveform is compatible with the existing services of the Space Network. Typically this waveform is used to send up to 100 Mbps over the return link SCA_N Testbed to ground via the TDRSS. A spectrum capture of the baseline waveform is shown in Figure 3. Note that the waveform fully occupies the 225 MHz channel allocation.

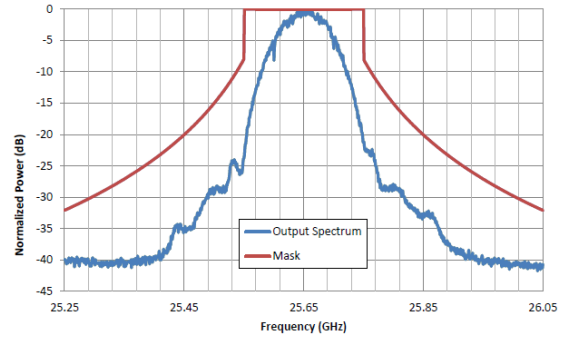


Figure 3. Baseline waveform spectrum with 225 MHz channel mask - 1/2 rate OQPSK at 100 Mbps user data.

IV. Bandwidth-Efficient Waveform

The *Reconfigurable Bandwidth-Efficient Waveform for High-Rate Telemetry* supports tunable data-rates up-to 1000 Mbps, and a modulation symbol rate up-to 200 MSymbols/second. The supported modulations include GMSK, BPSK, QPSK, OQPSK, 8-PSK, 16-APSK, 16-PSK, 16-QAM, and 32-APSK. Various pulse-shape filtering options are available, using Root-Raised Cosine and Raised Cosine filters, with excess bandwidths (parameter α) between 0.1 and 1.0. The supported forward error correction codes include Low Density Parity Check (LDPC) codes, specifically the AR4JA and C2 codes.⁹ From the AR4JA family, the waveform supports rates 1/2, 2/3, and 4/5 ($k = 1024$). From the C2 family, the waveform supports the rate 7/8 code. Additional data processing includes Consultative Committee for Space Data Systems (CCSDS) compliant randomization (131.0-B-2)⁹ and Advanced Orbiting Systems (AOS) data framing (732.0-B-2).¹⁰ All features (see Table 2) are available in the same waveform load with minimal time required to change the mode of operation. The waveform’s block diagram is shown in Figure 4.

Table 2. Waveform Summary

Module	Description
Data Source	External, or PRBS 9, 11, 15, 23, 31
User Data Rates	0.1 - 1000 Mbps (Un-coded)
Framing	CCSDS 732.0-B-2
Randomization	CCSDS 131.0-B-2
Forward Error Correction	LDPC Rate 1/2, 2/3, 4/5 (ARJ4A, $k=1k$), LDPC Rate 7/8 (C2, $k=7k$)
Modulation	GMSK, BPSK, QPSK, OQPSK, 8/16-PSK, 16/32-APSK, 16-QAM
Pulse-shape Filter	Square-Root Raised Cosine, Raised Cosine, Gaussian (GMSK only)
Digital Pre-distortion	Memory-less (Look-up Table and Symbol Position)
Channel Pre-compensation	32-tap Finite Impulse Response (FIR) Filter
Receiver Power Detection	Antenna Pointing Quality Metric (APQM) for Closed-Loop Tracking

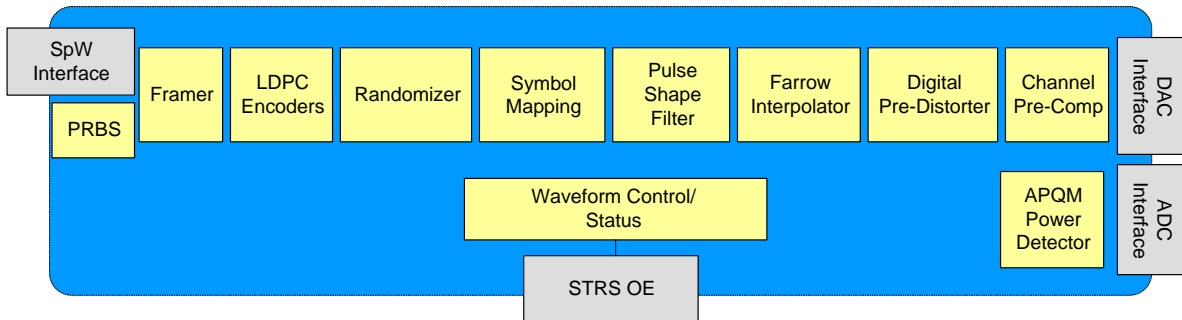


Figure 4. Waveform Functional Block Diagram

The GRC-developed waveform and the Harris SDR platform are compliant with the Space Telecommunications Radio System (STRS) standard, an open architecture standard for SDRs.¹² The waveform is available for future mission re-use via the STRS waveform repository.¹³

V. Test/Technology Objectives and Goals

The primary objective of this experiment is to maximize the data-rate over the Space Network’s Ka-band return link while using bandwidth-efficient techniques. Current practice in NASA’s Space Network for the Ka-band service is BPSK, QPSK, or Offset-QPSK modulation. The spectral efficiency of OQPSK is compared to several potential modulations in Table 3. As shown below, these modulations offer significant improvement in spectral efficiency over current practice. This will allow users to maximize the data throughput given the available spectrum.

Table 3. Spectral Efficiency Comparison

Modulation	Spectral Efficiency (b/s/Hz), 99%	Improvement Factor
OQPSK, Low-pass Filtered	0.59	-
Precoded GMSK, (BT=0.3)	1.1	1.86x
OQPSK, (SRRC 0.2)	1.77	3.0x
8-PSK, (SRRC 0.35)	2.57	4.36x
16-APSK, (SRRC 0.35)	3.43	5.8x
32-APSK, (SRRC 0.35)	4.39	7.44x

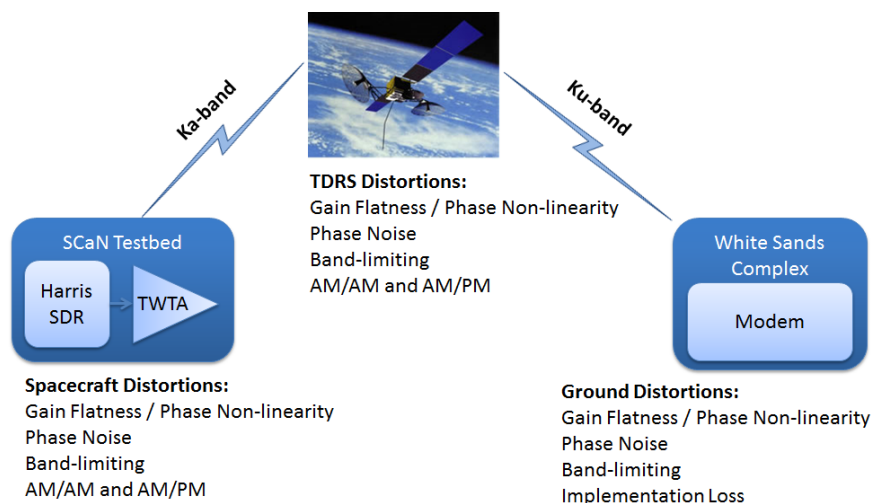


Figure 5. Communication system impairments over Ka-band relay satellite channel.

Additional objectives for the experiment include developing methods to compensate for the gain and phase distortions over the channel, including the nonlinear distortions from TWT amplifiers (Figure 5). Simulations of the TDRS channel have shown that the user spacecraft nonlinear phase and amplitude distortions from the TWTA are a significant factor in determining the overall system performance, especially with high-order modulations.¹¹ Compensation methods may be applied in the analog or digital domain, however, digital pre-distortion techniques are easy to implement when using SDRs. Implementing resource efficient pre-distortion techniques on the user-spacecraft will improve system bit-error-rate (BER) performance and power amplifier efficiency.

VI. Channel Predistortion

The spectral efficient modulations being demonstrated in this experiment, with the exception of GMSK, have non-constant power envelopes (i.e. peak-to-average ratio greater than 1). This necessitates backing-off the average power that is driving the TWTA, such that the peaks of the modulated waveform are not overly

compressed. The compression that occurs near saturation causes spectral regrowth and can degrade the BER performance over the link. It is desirable to minimize the amount of back-off so that the output power is maximized and the amplifier can operate near saturation where it is more power efficient. In this system the drive level into the TWTA is controlled digitally, by reducing the amplitude of the modulated waveform from the digital-to-analog converter (DAC). More advanced methods use pre-distortion algorithms to compensate for the nonlinear distortions, allowing for higher output power and minimal spectral re-growth.

SDRs can be programmed to implement digital pre-distortion (DPD) algorithms. DPD algorithms can range in complexity from simple, open-loop, compensation lookup tables (LUT) to high order memory polynomial models with closed-loop feedback. This experiment is focused on feed forward algorithms appropriate for resource-constrained space-qualified SDRs. Two DPD algorithms were selected for implementation on the SDR, lookup table and symbol position pre-distortion, and will be described in the following sections.

A. Lookup Table

The lookup table memoryless DPD algorithm functional diagram is shown in Figure 6. Complex samples from the modulator are used to calculate the instantaneous power of the waveform. The computed power is used to index a 256 element LUT that corresponds to the appropriate complex scaling coefficient. Coefficients in the LUT are computed from the mathematical inverse of the amplitude-dependent gain and phase characterization data for the amplifier. The current complex sample and the corresponding scaling coefficient are multiplied together to produce the pre-distorted waveform.

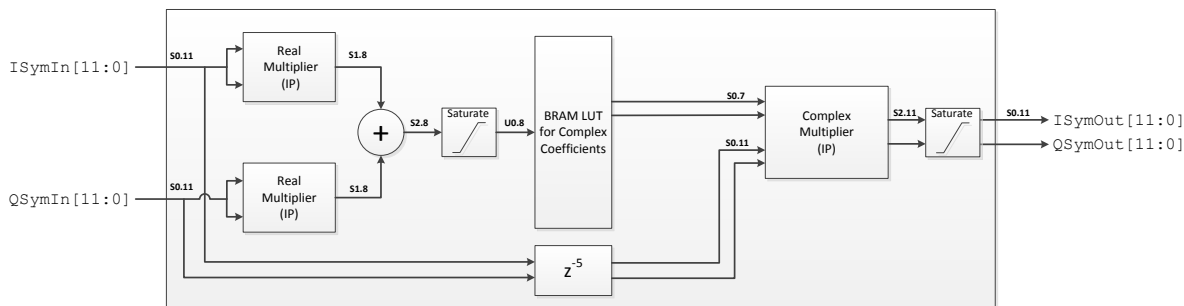


Figure 6. Lookup table DPD implementation in waveform.

B. Symbol Position

The symbol position DPD algorithm is currently applied to the 16-APSK modulation mode of the waveform. In this mode, the amplitude ratio and the relative phase between the inner and outer rings are adjusted in the waveform symbol mapper. This greatly simplifies fine tuning of the DPD algorithm compared to the LUT method as there are only two parameters to change. While the LUT mode is able to provide DPD across all modulation modes as well as compensate during transitions between symbols, this symbol position DPD method has been proven effective in testing for 16-APSK.

VII. Test Results

Test results are presented for three phases of testing. First, the system was tested in the laboratory with the Harris SDR breadboard or SCA_N Testbed engineering model to baseline performance and to determine key operation waveform parameters, such as optimal pulse-shape filter α and TWTA drive levels. Careful considerations were given to maximize output power while meeting obligations to the National Telecommunications and Information Administration (NTIA) for spectral emissions compliance. These tests include the waveform implementation and receiver loss, but do not include the impact of the TDRS channel. Section A summarizes key results of the ground testing. Next, as a precursor to the flight testing with SCA_N Testbed, the Harris SDR breadboard was transmitted through the TDRS channel using a ground terminal at White Sands Complex. This configuration did not include the impacts of the user spacecraft TWTA, but does include TDRS and the USS-CR modem equipment. Section B summarizes results from the end-to-end testing. Finally, the on-orbit flight testing with SCA_N Testbed is summarized in section C.

A. Ground Testing

1. Pulse-Shape Filter

A suite of BER tests were made to determine the optimal coefficients for the SRRC pulse-shape filter. Results for uncoded 8-PSK at 150 Mbaud showed that an α of 0.35, 0.5, and 1.0 performed similarly, and performance began to degrade by several dB for an α of 0.2 and lower. Therefore, an α of 0.35 appeared to be a good compromise between spectral efficiency and implementation loss. In order to meet the NTIA spectral mask for certain modes, an $\alpha = 0.2$ or lower is required at the highest symbol rates.

2. 16-APSK Digital Pre-Distortion

The symbol pre-distortion algorithm was evaluated with the 16-APSK mode operating at 150 Mbaud for a code word error rate (CWER) of 1e-6 at various TWTA drive levels. In Figure 8, it is shown that the total degradation of the system is minimized at 3 dB input back-off (IBO). IBO and output power back-off (OBO) are defined relative to the TWTA operating at saturation. In this implementation and waveform mode, the minimal total degradation is equivalent with or without DPD at the optimal IBO operating point. However, there is significant improvement in total degradation at lower IBO levels near saturation. It should be noted that the saturated drive level, and therefore the IBO, can change significantly over the full operating temperature range of the radio system. Thus, the use of DPD can reduce the impact of temperature on the communication system performance. Additional testing with 16-APSK mode configured with a LDPC 1/2 rate code showed ~ 0.25 dB improvement in total degradation when using DPD, implying that DPD performance and the optimal operating point can vary with code rate.

An interesting observation in Figure 8 is that past 7 dB IBO, the measured receiver implementation loss curve begins to gradually increase. This is believed to be caused by numerical fixed-point noise in the transmitted signal due to digitally backing off the signal power with the DAC. High-order modulations may benefit from an analog method of controlling signal power, to avoid losing DAC precision.

3. Optimal TWTA Drive Levels

Since GMSK is a constant envelope modulation, it was ran at saturation to maximize output power. For each of the remaining modulations in Table 4, BER curves were generated at various OBO operating points, and the drive level was chosen to minimize the total degradation of the system. Not all FEC code rates were evaluated. Due to time constraints, the optimal drive level for 32-APSK was

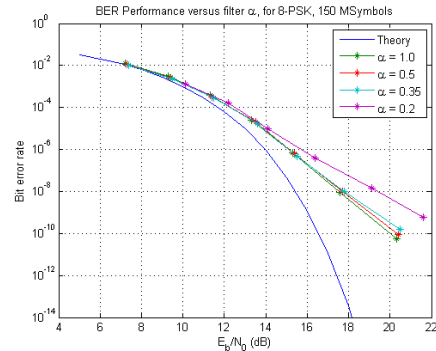


Figure 7. Harris SDR breadboard and Zodiac Receiver BER performance versus SRRC α .

Table 4. TWTA Drive Level per Waveform Mode, with SRRC $\alpha = 0.35$

Modulation	FEC	Mbaud	DPD	OBO
GMSK	All	150	N/A	0 (dB)
OQPSK	All	150	N/A	1.0 (dB)
8-PSK	All	150	N/A	1.0 (dB)
16-APSK	AR4JA 1/2	100	Off	1.0 (dB)
16-APSK	AR4JA 1/2	100	On	1.15 (dB)
16-APSK	C2 7/8	150	Off	1.3 (dB)
16-APSK	C2 7/8	150	On	1.45 (dB)

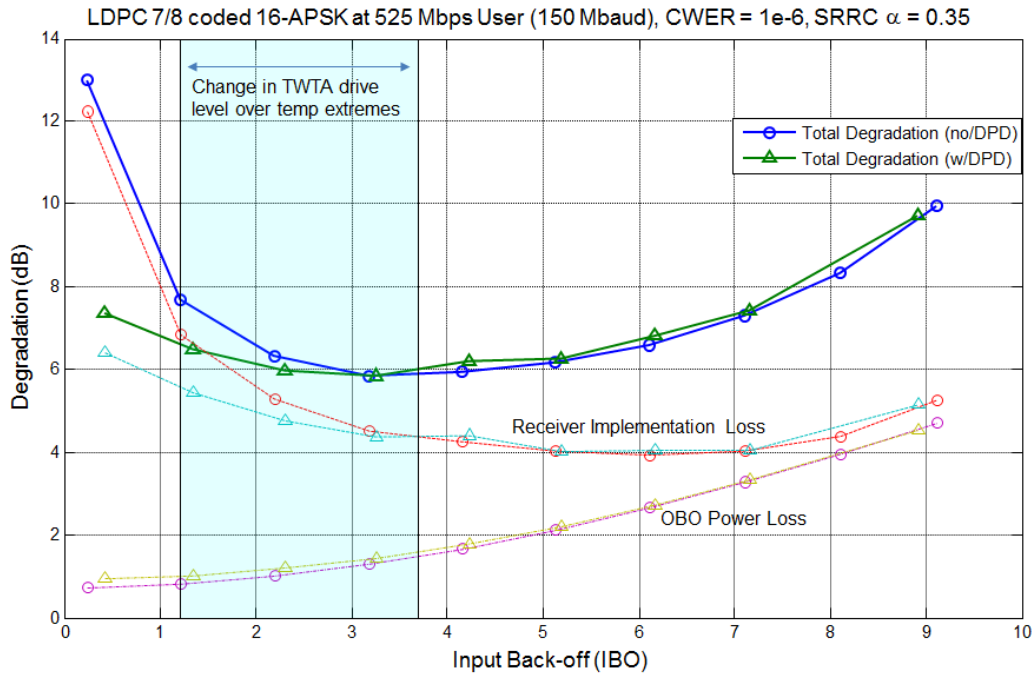


Figure 8. TWTA drive level optimization without DPD (○) and with DPD(△). Note that the total degradation is the summation of the receiver implementation loss and the OBO power loss.

not characterized. The drive level was controlled digitally by backing off the DAC signal power. Operationally, the DC power telemetry of the TWTA was used to estimate the resulting RF output power, based on device characterization curves.

4. 32-APSK Performance Characterization

Figure 9 presents preliminary CWER performance of 32-APSK with LDPC 7/8 encoding, demonstrating the full 200 Mbaud rate (1000 Mbps coded, 875 Mbps user information). Error bars are provided for 95% confidence intervals, following the recommended practices for coded curves.¹⁴ The results with the Ka-band TWTA included in the system show substantial degradations. Performance is expected to improve with DPD, optimal drive level determination, and evaluating other pulse-shape filter parameters in the bandlimited channel. Receiver acquisition was aided by training custom matched filters with QPSK, and then transitioning to 32-APSK. Also, note that due to the 9.3 dB IBO, additional degradation is expected from the loss of DAC precision.

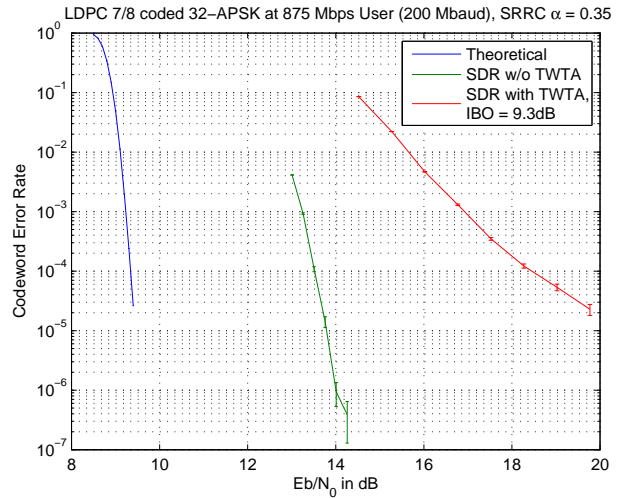


Figure 9. CWER Performance of 32-APSK LDPC 7/8.

B. TDRS End-to-End Testing

The end-to-end testset (EET) at WSC emulates a user spacecraft by providing a Ka-band uplink to TDRS via the standard Single Access (SA) service. The user spacecraft signal is relayed through the Ku-band downlink to the Second TDRS Ground Terminal (STGT) (Figure 10). For this test configuration, the Harris SDR breadboard is used as the transmitter, and interfaces with the EET at an IF of 370 MHz. The received signal from the IF service is provided to both the USS-CR WB Demodulator and the Zodiac High-rate Receiver. The EET configuration allows testing of waveforms under a stable environment, and can support higher carrier-to-noise density (C/N_0) levels than possible with the SCaN Testbed.

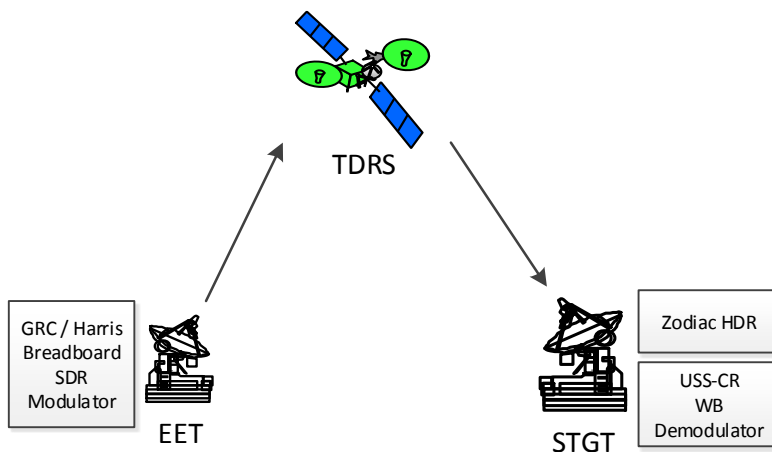


Figure 10. End-to-End Test Configuration.

Over the EET, 8-PSK with LDPC 7/8 encoding operated error free at full symbol rate (600 Mbps coded, 525 Mbps user information). The channel pre-compensation FIR filter of the waveform was used to correct for ~ 10 dB in gain-tilt in the Ka-band uplink equipment of the EET system. This gain-tilt was not observed in the flight testing. In either case, a steep increase in the receiver implementation loss was observed at the highest baud rates, as shown in Figure 11. This is presumed to be due to the band limiting channel. Due to time constraints, these curves were generated with only an $\alpha = 0.35$, better performance at the highest baud rates may be possible with a lower α . The corresponding C/N_0 threshold for the highest rate (with pre-compensation filter) is ~ 99.7 dB-Hz.

At a fixed C/N_0 of 103 dB-Hz, 16-APSK with LDPC 7/8 was able to achieve 775 Mbps over-the-air (~ 678 Mbps user information). A steep increase in the receiver implementation loss was observed at the highest baud rates, which prevented the 800 Mbps test case from acquiring. See Table 5 for details.

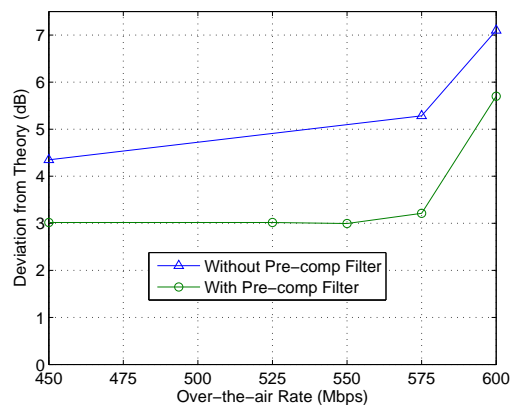


Figure 11. EET system loss versus data-rate for 8-PSK LDPC 7/8.

Table 5. 16-APSK with LDPC 7/8 Performance over the TDRS EET with $C/N_0 = 103$ dB-Hz

Over-the-air (Mbps)	User data rate (Mbps)	Coded BER	Uncoded BER	Eb/No Est.	Bits Received
750	656.25	~ 0	$7.5e-3$	9.2	$3e10$
775	678.125	$3e-9$	$8.4e-3$	8.9	$4e10$
800	700				<i>Did not acquire</i>

C. Flight Testing

Flight testing of the waveform consists of scheduled TDRS events, lasting 20-30 minutes, with SCaN Testbed on-board the ISS. The tests were designed to operate at the maximum data-rate supported, with minimal C/N_0 margin, to determine the operational bounds. During the flight testing campaign, the following modulations were tested: GMSK, OQPSK, 8-PSK, 16-APSK, and 32-APSK. The new pulse-shape filtered OQPSK mode showed a significant improvement over the baseline low-pass filtered OQPSK waveform and performed error free ($>1e11$ bits received) over numerous events using LDPC 7/8 at 200 Mbaud (350 Mbps user data rate). Uncoded GMSK also achieved error free ($>1e10$ bits received) communication up to 200 Mbaud (200 Mbps user data rate). For these modes, the channel bandwidth and SDR capabilities defined the performance bounds.

When testing with high-order modulations, the channel became C/N_0 limited and did not support error free operation with full baud rate. For the 8-PSK mode, the waveform generally performed error free ($>1e11$ bits received) for rates up to 150 Mbaud (393.75 Mbps user data rate), over multiple passes. Higher baud rates were tested with some BER degradation (Table 6), and required the use of custom matched filters on the receiver trained to the channel instead of the default SRRC with adaptive equalization. There were minor variations in the BER performance when using the same TDRS service due to path loss variations and different pointing losses between passes (see tests 1 & 2 and tests 3 & 4). The link was briefly operated at full symbol rate (see tests 6a and 6b) during the last portion of an event, but with poor BER ($1e-5$). The filter α was changed mid-test from 0.35 to 0.2, however, both modes had similar performance. Additional link margin is recommended to obtain reliable performance for these higher data rates, or additional compensation for the bandlimited channel response. Further testing with a filter α of 0.1 or 0.2 is also recommended.

Table 6. On-orbit 8-PSK with LDPC 7/8 Performance

Test	Coded rate (Mbps)	User rate (Mbps)	Filter α	BER	Bit Errors	Bits Received	Service
1	550	481.25	0.35	1e-8	9.6e3	9.6e11	TDW, SA1
2	550	481.25	0.35	3.4e-10	26	9.6e11	TDW, SA1
3	575	503.125	0.35	1e-5	a	a	TDW, SA1
4	575	503.125	0.35	2e-8	823	4e10	TDW, SA1
5	585	511.875	0.35	1e-9	33	3.3e10	TDE, SA1
6a	600	525	0.35	2e-5	5e5	2.5e10	TDE, SA1
6b	600	525	0.2	3e-5	8e5	2.7e10	TDE, SA1

The 16-APSK mode data rate was limited by C/N_0 , though more spectrally efficient. Error free performance was measured up to 150 Mbaud (Table 7) using 1/2 and 2/3 rate codes. The 7/8 rate code did not perform as well as the 1/2 and 2/3 codes in terms of error free peak user data rate. However, the 7/8 rate code was 1.67x more spectrally efficient than the 1/2 and 2/3 codes in delivering a ~ 250 Mbps user data rate.

Table 7. On-orbit 16-APSK performance with SRRC $\alpha=0.35$.

Test	Coded rate (Mbps)	User rate (Mbps)	LDPC rate	BER	Bit Errors	Bits Received	Service
7	500	250	1/2	~ 0	0	9.0e10	TDE, SA2
8	600	300	1/2	~ 0	0	1.0e11	TDW, SA2
9	600	400	2/3	~ 0	0	1.0e10	TDE, SA1
10	650	433.3	2/3	5e-8	750	1.0e10	TDE, SA1
11	300	262.5	7/8	~ 0	0	3e11	TDW, SA2
11	400	350	7/8	8e-5	a	a	TDE, SA1

The symbol position DPD algorithm was used with manual feedback (telephone exchange of ring ratio and phase parameters) between engineers at WSC observing receiver performance and engineers at the SCaN Testbed control center configuring the waveform parameters. This was an iterative un-optimized process, but easiest to implement with experiment schedule constraints. DPD improved acquisition and performance of 16-APSK significantly (Figure 12).

^aExact values for bit-errors and bits-received are available, but not recorded here for BER's worse than $1e-5$

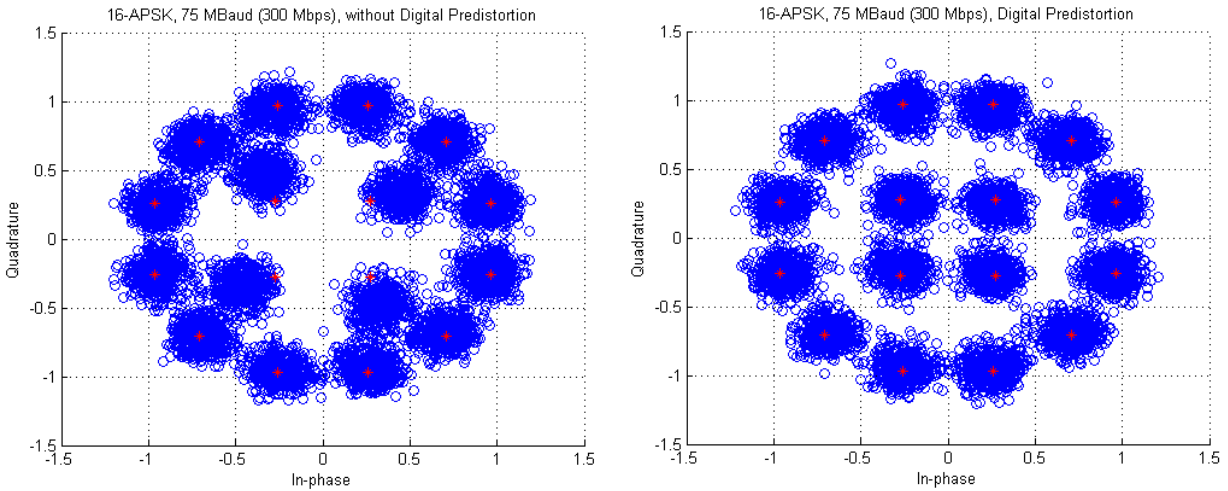


Figure 12. 16-APSK IQ constellation uncompensated (left) and with symbol position DPD (right).

For all high-order modulations, variations in equalizer performance was observed between the two high-rate receivers, especially in bandlimited channels. For the highest symbol rates (>180 Mbaud) the receivers struggled to obtain lock, especially at low margin. An iterative procedure was used to train up custom matched filters, instead of the SRRC matched filter. The same procedure was also applied to the TDRS end-to-end testing. The built-in adaptive equalizer was used to train the custom matched filter. After the custom matched channel filter was obtained, best performance was observed when disabling the adaptive equalizer algorithm, especially for bandlimited cases operating near threshold. As shown in Figure 13, the adaptive equalizer had unreliable performance, causing the receiver to go out of lock several times before being disabled. Figure 13 also shows the benefits of the DPD algorithm, in reducing the number of corrected errors / frame by a factor of 2.

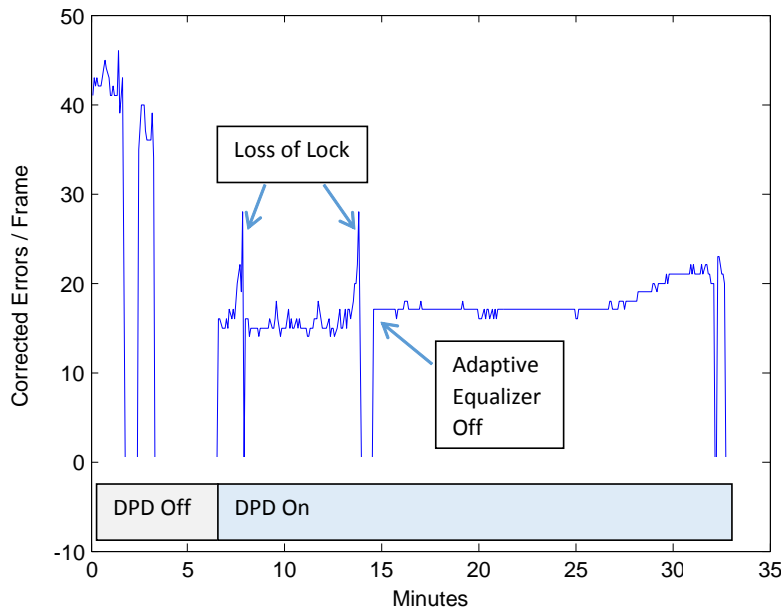


Figure 13. Corrected error per frame with and without DPD

VIII. Future Work

NASA is looking to improve the efficiency when using the communications and navigation infrastructure in the future by improving both spectrum utilization with more efficient waveforms such as the one described in this paper, and also improved asset utilization using techniques such as multiple access antennas, internetworking for improved data transport, store and forward data protocols (such as disruptive tolerant networking (DTN)) to efficiently move data through the network, and autonomy and cognition, with an emphasis on reducing user satellite resources (e.g. power, mass, cost) to improve overall system efficiency. As the TDRS system begins to approach its end of design lifetime in the 2025 through 2040 timeframe, NASA will deploy new relay satellites to continue its support to scientific research, robotics, and human exploration missions. The future architecture envisions allocating bandwidth from these new relay satellites on an as needed basis to different missions as compared to the circuit switched (single access) type of assignments made today. These future missions will rely on bandwidth efficient and adaptive waveforms.

The high-rate bandwidth-efficient waveform will be the basis of future waveforms which provide the needed flexibility to use different modulation and coding combinations with adaptive and cognitive applications. These cognitive applications will sense link conditions, environment, and system performance and choose configurations (frequency, modulation, coding, etc.) which will improve the efficiency and throughput of the communication links. Cognitive engines will employ reinforcement learning, supervised and unsupervised learning and other techniques to improve and optimize not only radio-to-radio link communications, but system wide efficiencies as well, for applications such as user satellites requesting and coordinating their own relay or direct to ground asset to send science data back to principal investigators and intelligent internetworking where data routes among network nodes according to the current and future (often dynamic) connectivity, data types, priority, and other event driven and learned conditions.

Finally, interoperability among infrastructure elements will be a key aspect enabled by new waveforms. Interoperability among waveforms implies compatibility with both commercial and international standards and among NASA, commercial, and international partner infrastructure (relays and ground stations). Interoperability improves the efficiency of using the communications infrastructure by providing services to missions of other countries, such as sharing a relay asset around Mars or the Moon or sharing a ground station on Earth among multiple deep space assets. The waveforms discussed here and the follow-on waveforms comply with various commercial (e.g. DVB-S2) and international (Consultative Committee for Space Data Standards CCSDS) standards.

New and advanced waveforms such as the high rate bandwidth efficient waveform discussed in this paper will improve and increase the data throughput from future missions. Waveforms that adapt to their environment, change their configuration, and work seamlessly across OSI layers will provide new information to science missions and improve mission efficiency going forward. Future work is to incorporate DPD automatic feedback control from the receiver back to the control center or more directly to the flight SDR via the forward link. Putting this DPD in the control of the SDRs along with other dynamically variable parameters (e.g. modulation and coding) is an enabling component of more advance cognitive communication systems.

IX. Conclusions

Due to an ever-increasing desire for more science data and the limited available spectrum, future missions will need to operate with bandwidth-efficient waveforms to maximize data throughput. This paper presented results of a high-rate, bandwidth-efficient experiment operating over the existing 225 MHz Ka-band service of the Space Network. Data-rates as high as 525 Mbps of user data were demonstrated on-orbit using the SCA_N Testbed, using high-order modulations, modern LPDC forward error codes, and pulse-shape filtered waveforms. Compared to the baseline OQPSK waveform with a rate 1/2 convolutional code, this experiment demonstrated a 5x increase in data-rate and spectral efficiency. Furthermore, this experiment explored methods for even higher efficiency, including 16-APSK and 32-APSK modulations. A simple digital-predistortion algorithm was implemented to improve performance of multi-level modulations (such as 16-APSK) in the presence of nonlinear channel distortions. Although the experiment results in this paper were for the relay satellite channel, they are also appropriate for direct-to-Earth links where there is reduced path loss and the potential for higher signal-to-noise ratios. Demonstrations of these new techniques on a realistic on-orbit flight experiment provided valuable experience and reduced the risk of using these techniques in future missions.

Acknowledgments

Special thanks to James Ruspoli, Mickey Flynn, and Josh Buchanan from White Sands Complex for supporting the tests, and the SCaN Testbed Operations team.

References

- ¹R. C. Reinhart, J.M Sankovic, S.K. Johnson, J.P. Lux, "Recent Successes and Future Plans for NASA's Space Communications and Navigation Testbed on the ISS", *International Space Station, 65th International Astronautical Congress*, Toronto, Canada, Sept. 2014.
- ²R. C. Reinhart, J.P. Lux, "Space-based Reconfigurable Software Defined Radio Test Bed aboard International Space Station", *SpaceOps Conference 2014*, Pasadena, California, May 2014.
- ³D. Chelmins, D.J. Mortensen, M.J. Shalkhauser, S.K. Johnson, R.C. Reinhart, "Lessons Learned in the first year operating Software Defined Radios in Space", *Space 2014 Conference*, Pasadena, California, Aug. 2014.
- ⁴J.A. Downey, R.C. Reinhart, T.J. Kacpura, "Pre-flight Testing and Performance of a Ka-band Software Defined Radio", *Space 2014 Conference*, Pasadena, California, Aug. 2014.
- ⁵Simons, R. N., Force, D. A., Spitsen, P. C., Menninger, W. L., Robbins, N. R., Dibb, D. R., Todd, P. C., High Efficiency K-Band Space Travelling-Wave Tube Amplifier for Near-Earth High Data Rate Communications NASA/TM-2010-216262, Glenn Research Center, Cleveland OH, March 2010.
- ⁶*Space Network User's Guide (SNUG)*, 450-SNUG Rev 10, Greenbelt, Maryland, Aug. 2012.
- ⁷M. Toral, J. Wesdock, A. Kassa, P. Pogorelc, "On-orbit Performance Verification and End-to-End Characterization of the TDRS-H Ka-band Communications Payload", *Eighth Ka-Band Utilization Conference*, Baveno/Stresa-Lake Maggiore, Italy, Sept. 2002
- ⁸H.C. Shaw, P.E. Boldosser, Y.F. Wong, D. D. Lakins, C. Shulman, J. Ramirez, Z. Johnson, J.W. Ozborn, C.S. Kozlowski, "TDRSS Space Ground Link Terminal Forestalls Obsolescence with Component Replacement and Upgrades", *SpaceOps 2012*, Stockholm, Sweden, 2012.
- ⁹*TM Space Data Link Protocol. Recommendation for Space Data System Standards*, CCSDS 132.0-B-1. Blue Book. Issue 1. Washington, D.C: CCSDS, September 2003.
- ¹⁰*AOS Space Data Link Protocol*, CCSDS 732.0-B-2. Blue Book. Issue 2. Washington, D.C: CCSDS, September, 2003.
- ¹¹B. Gioannini, Y. Wong, J. Wesdock, C. Patel, "Bandwidth Efficient Modulation and Coding Techniques for NASA's Existing Ku/Ka-band 225 MHz Wide Service", *IEEE Aerospace Conference*, Mar. 2005.
- ¹²*Space Telecommunications Radio System (STRS) Architecture Standard*, NASA-STD-4009 Baseline, <https://standards.nasa.gov/standard/nasa/nasa-std-4009>.
- ¹³<https://strs.grc.nasa.gov/repository/>.
- ¹⁴J. Hamkins, "Confidence Intervals for Error Rates Observed in Coded Communications Systems", IPN Progress Report 42-201, May 15, 2015